Journal of Zhejiang University SCIENCE A
ISSN 1673-565X (Print); ISSN 1862-1775 (Online)
www.zju.edu.cn/jzus; www.springerlink.com
E-mail: jzus@zju.edu.cn

# Detecting stable phase structures in EEG signals to classify brain activity amplitude patterns*

Yusely RUIZ[†1], Guang LI[†‡2], Walter J. FREEMAN[3], Eduardo GONZALEZ[1]

([1]*Department of Biomedical Engineering, Zhejiang University, Hangzhou 310027, China*)

([2]*National Lab of Industrial Control Technology, Institute of Cyber-Systems and Control, Zhejiang University, Hangzhou 310027, China*)

([3]*Department of Molecular & Cell Biology, 101 Donner University of California at Berkeley, CA 94720-3206, USA*)

[†]E-mail: yuselyrg79@yahoo.es; guangli@zju.edu.cn

Received Oct. 6, 2008; Revision accepted Feb. 11, 2009; Crosschecked Aug. 14, 2009

**Abstract:** Obtaining an electrocorticograms (ECoG) signal requires an invasive procedure in which brain activity is recorded from the cortical surface. In contrast, obtaining electroencephalograms (EEG) recordings requires the non-invasive procedure of recording the brain activity from the scalp surface, which allows EEG recordings to be performed more easily on healthy humans. In this work, a technique previously used to study spatial-temporal patterns of brain activity on animal ECoG was adapted for use on EEG. The main issues are centered on solving the problems introduced by the increment on the interelectrode distance and the procedure to detect stable frames. The results showed that spatial patterns of beta and gamma activity can also be extracted from the EEG signal by using stable frames as time markers for feature extraction. This adapted technique makes it possible to take advantage of the cognitive and phenomenological awareness of a normal healthy subject.

**Key words:** Electroencephalograms (EEG), Spatial-temporal pattern, Stable phase structure, Frames
**doi:**10.1631/jzus.A0820690 **Document code:** A **CLC number:** TP183; R741.04

## INTRODUCTION

Today there is increasing evidence that brain dynamics is self-organizing and scale-free (Stam *et al.*, 2003; Fingelkurts and Fingelkurts, 2001; 2004; Freeman, 2004a; 2004b; 2007a; 2007c). Several different techniques are currently used to describe brain activity on different scales: multiple spike activity (MSA) to describe microscopic activity, local field potentials (LFP) and electrocorticograms (ECoG) for mesoscopic activity, and electroencephalograms (EEG) and brain imaging (magnetoencephalography (MEG) and functional magnetic resonance image (fMRI)) for macroscopic activity. The action-perception cycle has been defined as the circular sequence from microscopic activity, which is evoked by receptor input from sensation, to macroscopic activity in concept formation and the reverse process dominates in motor cortices (Freeman, 2007a; 2007b; 2007c). In both cases, there are intermediate integration-differentiation processes on the mesoscopic scale that frequently yield ECoG spatial-temporal patterns with chaotic carrier waves in the beta or gamma range. These patterns are modulations in amplitude and phase (Freeman and van Dijk, 1987; Freeman and Barrie, 2000; Ohl *et al.*, 2000; Freeman and Burke, 2003; Freeman *et al.*, 2003; 2006a; 2006b).

Spatial-temporal patterns of ECoG signals have been classified with respect to conditioned stimuli (Lehmann *et al.*, 1998; Freeman and Barrie, 2000; Freeman, 2003; 2005; Freeman *et al.*, 2006a; 2006b). These patterns are described as stable frames with carrier frequencies in the beta or gamma band that recur at similar rates in the theta or alpha band (Fingelkurts and Fingelkurts, 2001; 2004; Freeman,

‡ Corresponding author

* Project supported by the National Natural Science Foundation of China (Nos. 60421002 and 60874098), and the National High-Tech Research and Development Program (863) of China (No. 2007AA04 2103)

2006). They emerge after sudden jumps in cortical activity called 'state transition' (Freeman, 2004a; 2006). Phase modulation (PM) patterns have a radial symmetry similar to that of a cone. The apex marks the nucleation site of the amplitude modulation (AM) patterns. AM patterns classified with respect to conditioned stimuli have been localized using the pragmatic information index (Freeman, 2005; 2006; 2007a) and identified with chaotic phase transitions (Kozma and Freeman, 2002).

Thus far ECoG recording has been used to study spatial-temporal patterns at the mesoscopic scale of brain electrical activity that is recorded directly from the cortical surface. On the one hand, it is an invasive procedure, and surgery is necessary to fix or remove the electrode array to or from the brain cortex. This procedure is commonly used with animals and occasionally with humans who have brain diseases that require surgery or are victims of global paralysis (Hinterberger *et al.*, 2003). On the other hand, EEG recording is a procedure in which electrical activity is recorded from the surface of the scalp through metal electrodes (Niedermeyer and Lopes da Silva, 2005). This is a completely non-invasive procedure that can be applied repeatedly to patients, normal adults, and children, with virtually no risk or limitation. Consequently, it is a research interest to adapt the techniques of ECoG to EEG to more easily detect and classify spatial-temporal patterns of brain activity.

In this paper, an EEG database that was previously used to study event related potentials (ERP) (Begleiter *et al.*, 1995; Zhang *et al.*, 1995; 1997) was employed to analyze the EEG from experiments trial by trial and to detect spatial amplitude patterns in EEG activity. Subjects had engaged in an object recognition task during the EEG recordings (Zhang *et al.*, 1995; 1997). Similar methods previously used to localize and classify AM patterns in ECoG (Barrie *et al.*, 1996; Kozma and Freeman, 2002; Freeman, 2004b; Freeman *et al.*, 2006b; Ruiz *et al.*, 2007) were applied to EEG. Owing to the well known differences in scale and resolution between ECoG and EEG, adjustments in the technique to identify stable frames and estimated frame gradient were necessary to make this method suitable for use with EEG signals. Stable frames were used as time markers to extract high-dimensional feature vectors. A multidimensional scaling technique of nonlinear mapping was applied to produce 2D visualization and to reduce the dimension of the feature vectors (Sammon, 1969; Freeman, 2005; 2006). Classification of these vectors was done using the back-propagation (BP) neural network.

Frames obtained from the EEG recording had similar characteristics and parameters to frames obtained from ECoG (Freeman, 2004b; Freeman *et al.*, 2006b). The mean level of classification for EEG was comparable to that for ECoG, higher than 75%, which shows for the first time that, owing to the scale-free properties of brain activity, these techniques adapted from ECoG can be employed to extract useful information noninvasively from scalp EEG.

## DATA SELECTION AND PREPROCESSING

The data used in this work were available from Ingber (1999). The data consist of a set of measurements from 64 electrodes placed on a scalp at standard sites (AEA, 1990) as shown in Fig.1. The sample rate was 256 Hz and the signal duration was 1 s. All scalp electrodes were referred to as Cz. The signals were amplified with a gain of 10 000 by Ep-A2 amplifiers with a band pass between 0.02 and 50 Hz, and recorded on a concurrent 55/50 computer. Trials with excessive eye and body movements (>73.3 μV) were rejected on-line.

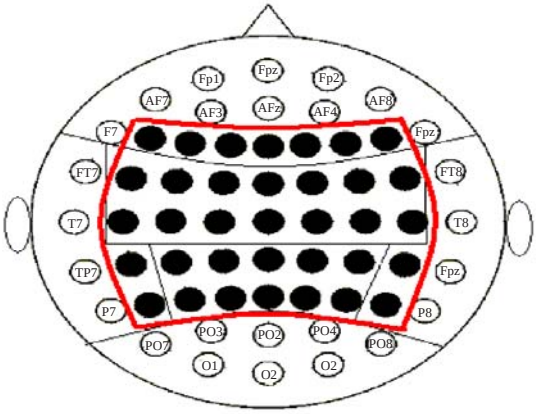


**Fig.1 Location of the 64-electrode array**
For these experiments, a subset of 35 electrodes was selected (black dots)

A set of figures from the Snodgrass and Vanderwart (1980) picture set were chosen as stimuli. During the experiments, each subject was exposed to

either a single stimulus (S1) to become familiar with the figures, or two stimuli (S1 and S2) to perform a recognition task. The two stimuli were displayed in either a matched condition (S1 was identical to S2) or a non-matched condition (S1 differed from S2).The subject's task was to decide whether or not the second picture (S2) was identical to the first stimulus (S1). After the presentation of S2 on each trial, the subjects were asked to press a mouse button in one hand if S2 matched S1 and to press a mouse button in the other hand if S2 differed from S1. All figures selected as stimuli represented a different concrete object and were easily identifiable. The stimuli were presented on a white background at the center of a computer monitor. The picture size ranged from 5 to 10 cm in height and 5 to 10 cm in width, and they were displayed for 300 ms.

The database consists of recordings from two groups: alcoholic subjects and control subjects (with no symptoms of alcoholism or other diseases). In this work, in order to have normal EEG to use for analysis, only recordings from the control subjects were used to carry out the experiments.

Recordings from each control subject were visually inspected to select an appropriate set of recordings for analysis. All subjects with fewer than 20 trials per stimulus or more than 3 noisy channels were rejected; a total of 14 subjects were finally selected. With the aim of avoiding electromyographic noise, an array of 35 electrodes, which mainly consisted of the frontoparietal electrodes, were selected (Fig.1).

The raw EEG data were visually inspected, and bad channels were replaced by the mean of the adjacent channels. The signals were then demeaned and normalized (Freeman, 2005). The temporal power spectral density (PSD) was estimated for each channel and then averaged for each trial and subject. A temporal band pass filter was applied to select the frequency range of interest (Freeman, 2004a; 2004b; 2005; 2006) prior to the application of the Hilbert transform (HT).

## AMPLITUDE MODULATION PATTERNS LOCATION

The Hilbert transform was used to obtain the analytic amplitude and analytic phase of the EEG signals (Barlow, 1993; Freeman, 2004a; 2004b). The analytic phase was used to calculate the parameters of instantaneous frequency and instantaneous gradient. These parameters were used to detect stable frames and estimate the other parameters of frames (Freeman, 2004b; Freeman *et al.*, 2006a; 2006b). AM patterns were observed during the time samples turned out by stable frames. The feature vectors were selected as the root-mean square (rms) values of the analytic amplitude within stable frames on the 35 electrodes. The 35-dimensional features were then transformed to a 2D feature vector using Sammon maps (Sammon, 1969; Freeman, 2005; 2006).

### Detecting stable frames

Cone fitting and spatial-temporal covariance methods have been used in the past to detect frames with similar results (Freeman, 2004b; Freeman *et al.*, 2006b; Ruiz *et al.*, 2007). Thus, using the spatial-temporal covariance method, thresholds for analytic phase covariance ($t_{e1}$) and analytic amplitude covariance ($t_{e2}$) were set. A time sample phase was selected as a frame candidate only if the analytic phase covariance was lower than $t_{e1}$, the analytic amplitude covariance was higher than $t_{e2}$, the sign of the instantaneous gradient did not change from one sample to the next, and the instantaneous frequency was within the temporal band used.

Between the time points when frame candidates were detected, the frame frequency and gradient were calculated by Eqs.(1) and (2):

$$F_N = \frac{1}{n}\sum_{i=1}^{n} w_i(t_n), \tag{1}$$

$$\gamma_N = \frac{1}{n}\sum_{i=1}^{n} \gamma(t_n), \tag{2}$$

where $n$ was the number of time steps across which a stable frame had been defined, $w_i$ was the instantaneous frequency and $\gamma$ was the instantaneous gradient. Other parameters, such as the frame phase velocity and frame diameter (Eqs.(3) and (4)), were derived from these two equations (Freeman, 2004b; Freeman *et al.*, 2006b). The frame rate was defined as the inverse of the time lapse between successive starting points of stable frames, and the duration was given by the number of digitizing steps over which the stable

frame was detected.

$$B = 2\pi F_N / (1000|\gamma_N|), \quad (3)$$

$$D_x = \pi / (2|\gamma_N|). \quad (4)$$

After that, supplemental, anatomical, and physiological evaluations were made of the acceptable parameter rank to exclude spurious frames from the analysis. The phase velocity had to be within the range of conduction velocities of cortical axons (1~10 m/s), the frame duration should have been more than 15 ms on the beta band or 10 ms on the gamma band, and the frame diameter had to be smaller than the width of the cerebrum, 200 mm (Freeman, 2004b; Freeman *et al.*, 2006b).

**Estimating instantaneous frequency and gradient**

Instantaneous frequency, or the rate of change in phase with time (Hz), was estimated as the successive differences of the unwrapped analytic phase divided by the digitizing step (Freeman, 2004b; Freeman *et al.*, 2006a; 2006b). This parameter is not interelectrode distance dependent.

On the other hand, instantaneous gradient, the rate of change in phase with distance (rad/mm), is interelectrode distance dependent. The interelectrode distance in previous work was in the order of 3 mm (Barrie *et al.*, 1996; Freeman *et al.*, 2006a; 2006b). For EEG, the interelectrode distance was increased to the order of 3 cm (Zhang *et al.*, 1995), but the analytic phase values are between $-p_i$ and $p_i$ rad in both cases (Barlow, 1993). The analytic phase differences are lower than $2p_i$ rad regardless of whether the interelectrode distance measures in millimeters, centimeters, or meters. Also, within the time period when the stable frames show up, the phase should be smooth and with little change from one electrode to another and from one time sample to the next, which produces very low analytic phase differences.

For ECoG, cone fitting was normally used to estimate the instantaneous gradient (Freeman and Barrie, 2000; Freeman and Rogers, 2003; Freeman, 2004b; Freeman *et al.*, 2006a; 2006b), but it is a highly time-consuming method and has technical constraints, which make it difficult to apply to EEG signals (Freeman, 2004b; Freeman *et al.*, 2006a). In Ruiz *et al.*(2007), a new method to estimate the instantaneous gradient was presented. In this method, the instantaneous gradient was estimated as the slope (m) of the line fitted to the differences between every analytic phase value and the other phase values for each interelectrode distance (Fig.2a). The results obtained were similar to the results produced by the cone fitting method (Ruiz *et al.*, 2007).

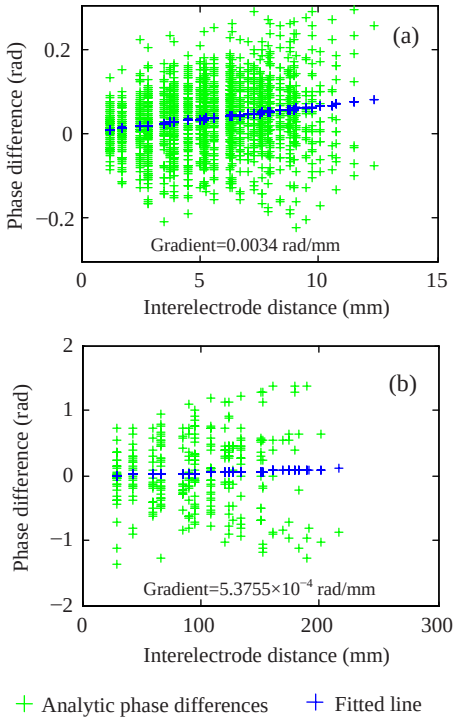


**Fig.2 Instantaneous gradient estimation**

(a) 64 channels of ECoG; (b) 35 channels of EEG. Gradients were estimated as the slope of the line fitted to the difference between every analytic phase value and the other phase values for each interelectrode distance. Due to the increase in the interelectrode distance, the gradient of the EEG signal was very low, which caused the frame velocity to be out of the range of the conduction velocity for the cortex. This example is from a signal filtered on the beta range, 12~30 Hz

The slope of one line is the relation between the variation in the *Y* axis (phase difference) and *X* axis (interelectrode distance) for two points. Due to the increase in the interelectrode distance, the gradient values for EEG were drastically reduced, even though the phase differences between electrodes had increased (Fig.2). Gradient values estimated using this method induced frame velocities higher than 150 m/s, and after the physiological criterion for frame detection were applied (Freeman, 2004b; Freeman *et al.*, 2006a; 2006b), no stable frames were detected. For

that reason, some changes in the gradient estimation method were made. The global instantaneous gradient was estimated as the slope of the line between the electrodes of the minimum and maximum phases for each time sample (Fig.3). The frame velocity estimated using this method was within the range of conduction velocity for the cortex, i.e., <10 m/s.

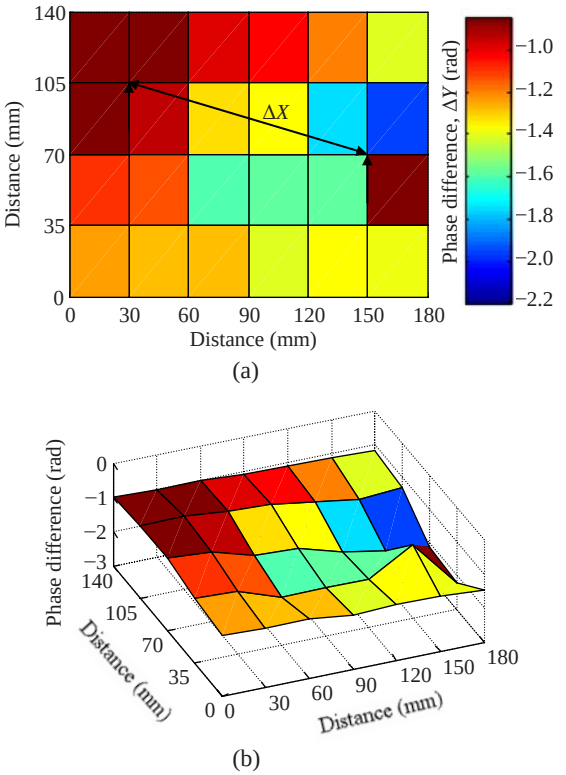


**Fig.3 Phase value on each electrode at one time sample**
(a) 2D view (b) 3D view. A global gradient (rad/mm) index was estimated for EEG signals as the slope of the line between the points of minima and maxima phase for each time sample. This example is from a signal filtered on the beta range, 12~30 Hz

## CLASSIFICATION PROCESS

Two classes were defined to carry out the classification process. The single-stimulus presentation was defined as class 1 and the two-stimulus presentation as class 2. Class 2 presentations can be in a matched condition (the first stimulus is identical to the second stimulus) or in a non-matched condition (the first stimulus is different from the second stimulus).

The Sammon map iteratively mapped the location of points defined from a high-dimensional (here 35-dimensional) space to a low-dimensional (here 2D) space, preserving the relative distances between points (Sammon, 1969; Freeman, 2005; 2006). After mapping, the feature vectors were labeled for graphic display and classification. BP networks were used to perform the classification.

Two-layer BP networks were used on linearly separable problems. Alternatively, if the problem required a boundary region other than a line, a three-layer BP was used to define it (Duda *et al.*, 2000; MATLAB user guide R2007b, http://www.mathworks.com). Two- and three-layer BP networks were used for classification (Fig.4). The training set consisted of 6 trials per class, and the test set conformed to all trials. The number of neurons in the hidden layer varied from 3 to 7, and the best performance was achieved with 5 neurons.

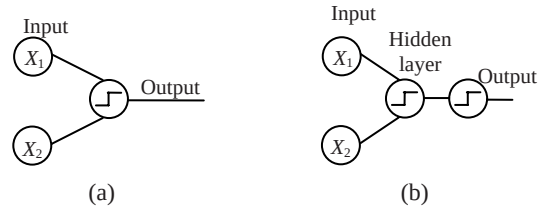


**Fig.4 (a) Two- and (b) three-layer BP networks were used in classification**
(a) was used on linearly separable problems and (b) on non-linearly separable problems

## RESULTS

The EEG signals were band pass filtered between 0.02 and 50 Hz during the recording process. Only the frequencies between 4 and 50 Hz were analyzed. Fig.5 shows an example of PSD displayed in log-log coordinates. PSD revealed a $1/f^{\alpha}$ form with upward deviations from a straight line in the frequency range from 10 to 45 Hz, and $\alpha$ varied from −1 to −3 (Freeman, 2004a; Freeman *et al.*, 2006b).

Frequencies from 12 to 30 Hz (beta band) and 30 to 45 Hz (low gamma) were used as the temporal band filter settings. Stable frame parameters were estimated for each subject and each class on the beta and gamma bands.

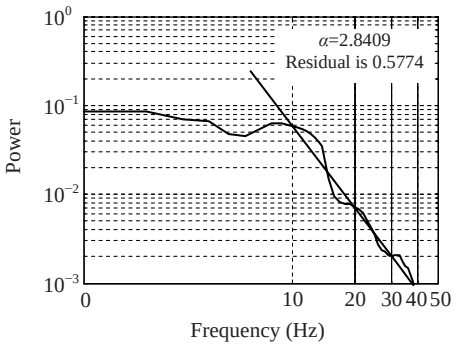


**Fig.5 PSD revealed a $1/f^{\alpha}$ form with upward deviations in the beta and gamma ranges, and $\alpha$ varied from −1 to −3**

Fig.6 shows the mean frame parameter value of each subject. Frequency, velocity, and duration were clearly distinguishable from frames on the beta or gamma band. Gradient, diameter, and rate values overlapped for some subjects. In general, stable frames from the beta band had lower carrier frequencies, velocities, diameters, rates, and a longer duration than stable frames on the gamma band did. The differences of stable frame parameters between classes were not obvious.

Feature vectors were extracted as the rms values of analytic amplitude on each electrode within the time periods where stable frames were detected. Sammon maps were used to visualize the distribution of the features (Fig.7) and to transform the 35-dimensional feature vectors into 2D feature vectors. Comparable maps were obtained from the beta and gamma bands, so only a few maps from the beta band are presented here.

Clusters of vectors were distinctly formed for almost all subjects. A line was drawn in the display plane between the clusters on the premise of linear separability, showing that the line almost separates the classes for some subjects but not for others. Because of this, a three-layer BP neural network was used for classification as well. Fig.8 shows the correct classification rate (CC) in percent per subject for a two-layer and a three-layer BP network.

The correct classification rate of beta and gamma patterns was around 70% using a two-layer BP network for almost all subjects and around 80% using a three-layer BP network. The three-layer BP network improved the mean classification rate by about 5% because for some subjects the clusters were well defined and the best boundary region was a line.

Correct classification rates that were higher than 62.5% for all subjects show that spatial patterns of beta and gamma activities can be extracted from the EEG signal. Differences between subjects can be ascribed to subjects' previous experiences, level of attentiveness, and level of expectation prior to the presentation of the stimulus (Freeman, 2004a; 2005; 2006).

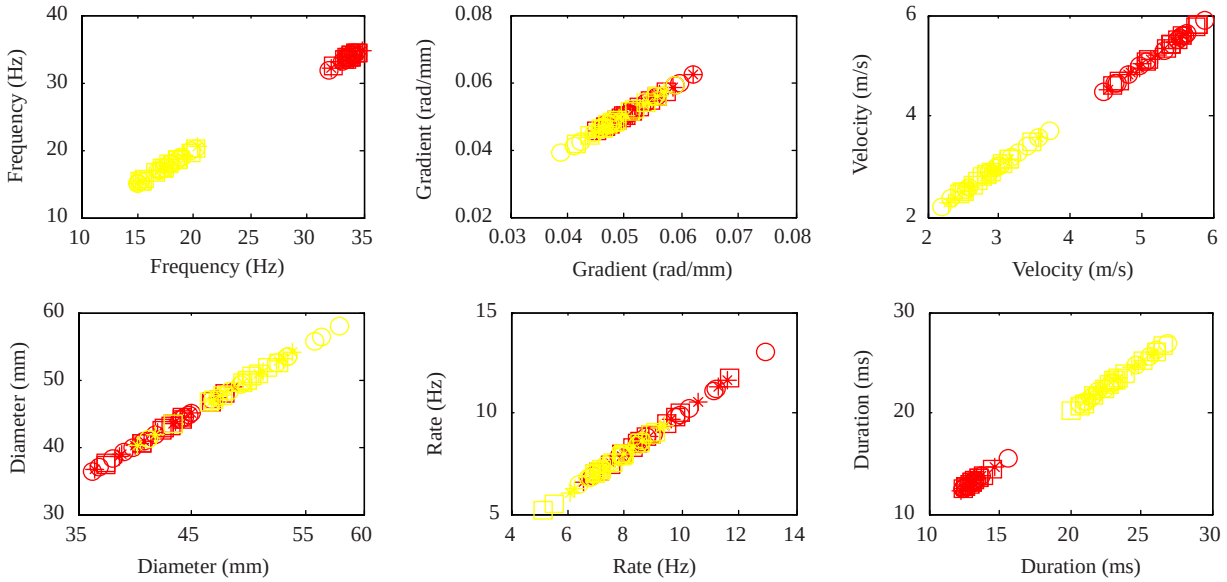


**Fig.6 Stable frame parameters on beta (light) and gamma (dark) bands for each class**

Asterisk, class 1; circle, class 2 matched condition; square, class 2 non-matched condition. Stable frame parameters for each band were clearly distinguishable, but no differences in frame parameters were observed within the classes on the same band

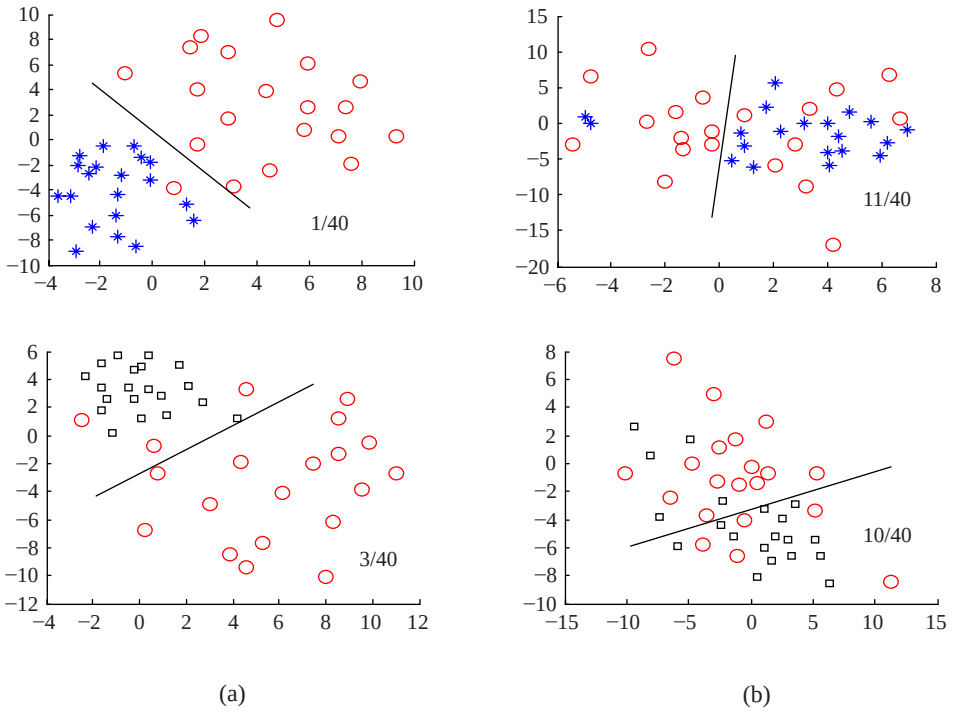


**Fig.7 Sammon maps of the feature vectors**

(a) Subject c344; (b) Subject co2c347. Sammon maps allow for the visualization of the feature vectors in 2D space. Top: class 1 (circle) vs class 2 matched condition (asterisk), bottom: class 1 (circle) vs class 2 non-matched condition (square), on beta band. A line was drawn to separate clusters and features positioned on the wrong side of the calculated line

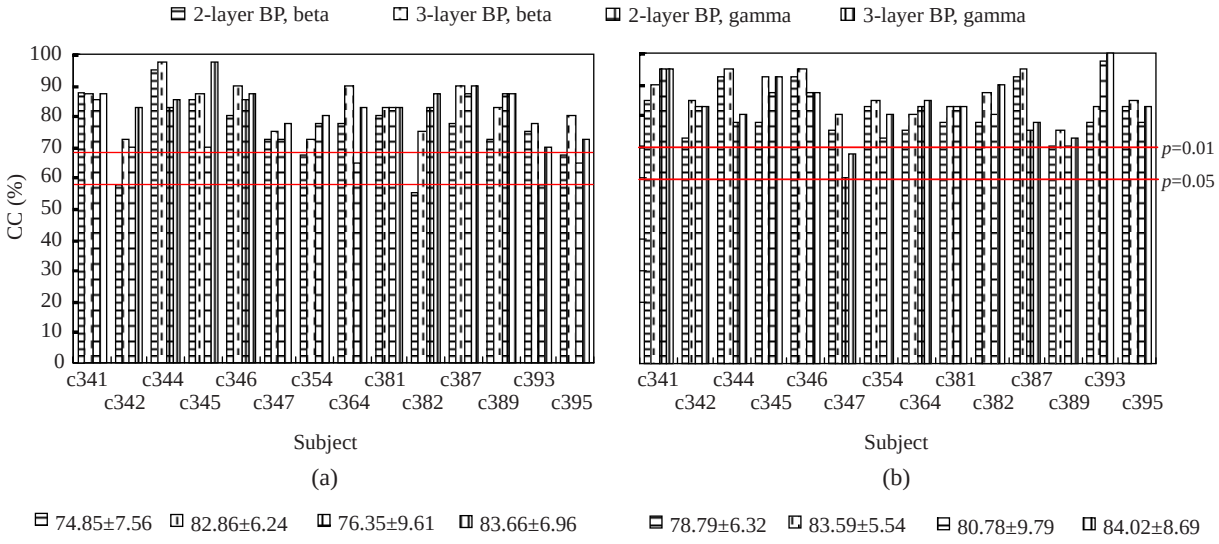


**Fig.8 Classification rate in (a) class 1 and class 2 matched condition and (b) class 1 and class 2 non-matched condition**

At the bottom '±' means the standard error of classification across all subjects. The 3-layer BP network improved the mean classification rate by around 5%

## CONCLUSION

Phase transitions that preceded the emergence of AM and PM modulation patterns were detected using the covariance method (Ruiz *et al.*, 2007). The global gradient estimation was used to detect stable frames and these stable frames were used as the time marker for feature extraction.

The hyperspace feature vectors were mapped into 2D space to display clusters of points that represent the differing spatial patterns corresponding to both the single-stimulus presentation and the double-stimulus presentation. The 2D space feature vectors were used for classification of these patterns.

Similar CC values were obtained for patterns on the beta and gamma bands. The CC was higher than 62.5% for all subjects ($p$=0.05 for binary classification), which shows that spatial patterns of beta and gamma activities can also be extracted from the EEG signal using this adapted technique.

This adapted technique can provide the foundation needed to investigate the cerebral dynamics of learning. It also allows researchers to take advantage of the cognitive and phenomenological awareness of a normal healthy subject and their verbal description of mental states by using a non-invasive technique to record the brain's electrical activity.

Previous studies have shown that phase transitions are different according to the temporal band pass selected. Future studies of frequency bands and bandwidth carrying levels of meaningful information should be done.

## ACKNOWLEDGEMENTS

The human data were collected by Henri Begleiter and associates at the Neurodynamics Laboratory at the State University of New York Health Center at Brooklyn and prepared by David Chorlian.

## References

AEA (American Electroencephalographic Association), 1990. Standard Electrode Position Nomenclature.

Barlow, J.S., 1993. The Electroencephalogram: Its Patterns and Origins. MIT Press, Cambridge, MA.

Barrie, J.M., Freeman, W.J., Lenhart, M.D., 1996. Spatiotemporal analysis of prepyriform, visual, auditory, and somesthetic surface EEGs in trained rabbits. *J. Neurophysiol.*, **76**(1):520-539.

Begleiter, H., Porjesz, B., Wang, W., 1995. Event-related brain potentials differentiate priming and recognition to familiar and unfamiliar faces. *Electroencephalogr. Clin. Neurophysiol.*, **94**(1):41-49. [doi:10.1016/0013-4694(94)00240-L]

Duda, R.O., Hart, P.E., Stork, D.G., 2000. Pattern Classification. John Wiley & Sons, New York. [doi:10.1007/s00357-007-0015-9]

Fingelkurts, A.A., Fingelkurts, A.A., 2001. Operational architectonics of the human brain biopotential field: towards solving the mind-brain problem. *Brain & Mind*, **2**(3):261-296. [doi:10.1023/A:1014427822738]

Fingelkurts, A.A., Fingelkurts, A.A., 2004. Making complexity simpler: multivariability and metastability in the brain. *Int. J. Neurosci.*, **114**(7):843-862. [doi:10.1080/00207450490450046]

Freeman, W.J., 2003. A neurobiological theory of meaning in perception: Part II. Spatial patterns of phase in gamma EEGs from primary sensory cortices reveal the dynamics of mesoscopic wave packets. *Int. J. Bifurc. Chaos*, **13**(9):2513-2535. [doi:10.1142/S0218127403008156]

Freeman, W.J., 2004a. Origin, structure, and role of background EEG activity: Part 1. Analytic amplitude. *Clin. Neurophysiol.*, **115**(9):2077-2088. [doi:10.1016/j.clinph.2004.02.029]

Freeman, W.J., 2004b. Origin, structure, and role of background EEG activity: Part 2. Analytic phase. *Clin. Neurophysiol.*, **115**(9):2089-2107. [doi:10.1016/j.clinph.2004.02.028]

Freeman, W.J., 2005. Origin, structure, and role of background EEG activity: Part 3. Neural frame classification. *Clin. Neurophysiol.*, **116**(5):1118-1129. [doi:10.1016/j.clinph.2004.12.023]

Freeman, W.J., 2006. A cinematographic hypothesis of cortical dynamics in perception. *Int. J. Psychophysiol.*, **60**(2):149-161. [doi:10.1016/j.ijpsycho.2005.12.009]

Freeman, W.J., 2007a. Definitions of state variables and state space for brain-computer interface: Part 2. Extraction and classification of features vectors. *Cogn. Neurodynam.*, **1**(2):85-96. [doi:10.1007/s11571-006-9002-9]

Freeman, W.J., 2007b. Proposed Cortical "Shutter" Mechanism in Cinematographic Perception. *In*: Perlovsky, L.I., Kozma, R. (Eds.), Neurodynamics of Cognition and Consciousness, p.11-38. [doi:10.1007/978-3-540-73267-9]

Freeman, W.J., 2007c. Definitions of state variables and state space for brain-computer interface: Part 1. Multiple hierarchical levels of brain function. *Cogn. Neurodynam.*, **1**(1):3-14. [doi:10.1007/s11571-006-9001-x]

Freeman, W.J., Barrie, J.M., 2000. Analysis of spatial patterns of phase in neocortical gamma EEGs in rabbit. *J. Neurophysiol.*, **84**(3):1266-1278.

Freeman, W.J., Burke, B.C., 2003. A neurobiological theory of meaning in perception: Part IV. Multicortical patterns of amplitude modulation in gamma EEG. *Int. J. Bifurc. Chaos*, **13**(10):2857-2866. [doi:10.1142/S0218127403008302]

Freeman, W.J., Rogers, L.J., 2003. A neurobiological theory of meaning in perception: Part V. Multicortical patterns of phase modulation in gamma EEG. *Int. J. Bifurc. Chaos*, **13**(10):2867-2887. [doi:10.1142/S0218127403008296]

Freeman, W.J., van Dijk, B.W., 1987. Spatial patterns of visual cortical fast EEG during conditioned reflex in a rhesus monkey. *Brain Res.*, **422**(2):267-276. [doi:10.1016/0006-8993(87)90933-4]

Freeman, W.J., Burke, B.C., Holmes, M.D., 2003. Aperiodic phase re-setting in scalp EEG of beta-gamma oscillations by state transitions at alpha-theta rates. *Hum. Brain Map.*, **19**(4):248-272. [doi:10.1002/hbm.10120]

Freeman, W.J., Holmes, M.D., West, G.A., Vanhatalo, S., 2006a. Dynamics of human neocortex that optimizes its stability and flexibility. *Int. J. Intell. Syst.*, **21**(9):881-901. [doi:10.1002/int.20167]

Freeman, W.J., Holmes, M.D., West, G.A., Vanhatalo, S., 2006b. Fine spatiotemporal structure of phase in human intracranial EEG. *Clin. Neurophysiol.*, **117**(6):1228-1243. [doi:10.1016/j.clinph.2006.03.012]

Hinterberger, T., Kübler, A., Kaiser, J., Neumann, N., Birbaumer, N., 2003. A brain-computer interface (BCI) for the locked-in: comparison of different EEG classifications for the thought translation device. *Clin. Neurophysiol.*, **114**(3):416-425. [doi:10.1016/S1388-2457(02)00411-X]

Ingber, L., 1999. EEG Database. Available from http://kdd.ics.uci.edu/databases/eeg/eeg.html

Kozma, R., Freeman, W.J., 2002. Classification of EEG patterns using nonlinear dynamics and identifying chaotic phase transitions. *Neurocomputing*, **44-46**(1-4):1107-1112. [doi:10.1016/S0925-2312(02)00429-0]

Lehmann, D., Strik, W.K., Henggeler, B., Koenig, T., Koukkou, M., 1998. Brain electric microstates and momentary conscious mind states as building blocks of spontaneous thinking: I. Visual imagery and abstract thoughts. *Int. J. Psychophysiol.*, **29**(1):1-11. [doi:10.1016/S0167-8760(97)00098-6]

Niedermeyer, E., Lopes da Silva, F. (Eds.), 2005. Electroencephalography: Basic Principles, Clinical Applications and Related Fields. Lippincott Williams & Wilkins, Baltimore.

Ohl, F.W., Schulze, H., Scheich, H., Freeman, W.J., 2000. Spatial representation of frequency-modulated tones in gerbil auditory cortex revealed by epidural electrocorticography. *J. Physiol.-Paris*, **94**(5-6):549-554. [doi:10.1016/S0928-4257(00)01091-3]

Ruiz, Y., Li, G., Freeman, W.J., Moreira, E.G., 2007. A New Approach to Detect Stable Phase Structure in High Density EEG Signals. Proc. 1st Int. Conf. on Cognitive Neurodynamics, p.741-745. [doi:10.1007/978-1-4020-8387-7]

Sammon, J.W., 1969. A nonlinear mapping for data structure analysis. *IEEE Trans. Comput.*, **18**(5):401-409. [doi:10.1109/T-C.1969.222678]

Snodgrass, J.G., Vanderwart, M., 1980. A standardized set of 260 pictures: norms for name agreement, image agreement, familiarity, and visual complexity. *J. Exp. Psychol.: Hum. Learn. Mem.*, **6**(2):174-215. [doi:10.1037/0278-7393.6.2.174]

Stam, C.J., Breakspear, M., Cappellen, A., Dijk, B.W., 2003. Nonlinear synchronization in EEG and whole-head MEG recordings of healthy subjects. *Hum. Brain Map.*, **19**(2):63-78. [doi:10.1002/hbm.10106]

Zhang, X.L., Begleiter, H., Porjesz, B., Wang, W., Litke, A., 1995. Event related potentials during object recognition tasks. *Brain Res. Bull.*, **38**(6):531-538. [doi:10.1016/0361-9230(95)02023-5]

Zhang, X.L., Begleiter, H., Porjesz, B., Litke, A., 1997. Visual object priming differs from visual word priming: an ERP study. *Electroencephalogr. Clin. Neurophysiol.*, **102**(3):200-215. [doi:10.1016/S0013-4694(96)95172-3]